

Effects of Recycled Aggregate Content on Pervious Concrete Performance

Lei Guo^{1,2,3}, Zi Guan¹, Lixia Guo^{1,2,3,*}, Weiping Shen¹, Zhilong Xue¹, Pingping Chen¹ and Mingru Li¹

¹School of Water Conservancy, North China University of Water Resources and Electric Power, Zhengzhou, 450046, China

²Henan Water Valley Research Institute, Zhengzhou, 450046, China

³Henan Key Laboratory of Water Environment Simulation and Treatment, Zhengzhou, 450002, China

*Corresponding Author: Lixia Guo. Email: guolx@126.com

Received: 05 August 2020; Accepted: 02 September 2020

Abstract: A recycled aggregate (RA) was prepared by crushing and sieving demolished discarded concrete pavements and was subsequently tested and analyzed to determine its various physical properties. On this basis, pervious concrete (PC) mix proportions were designed. Coarse RA particles with sizes of 5–10 and 10–20 mm were selected. Concrete specimens were prepared with a water–cement ratio of 0.3, an aggregate–cement ratio of 4.5, the substitute rates of RA with 0, 25%, 50%, 75% and a single-/double-gap-graded RA mix (mass ratio of particles with sizes of 5–10 mm to particles with sizes of 10–20 mm: 1:1, 1:2, 2:1, 2:3 and 3:2). Various properties of the RA-containing PC(RPC) were determined by analyzing the compressive strength, splitting tensile strength, effective porosity, permeation coefficient and impact and abrasion resistance of the specimens. The results showed the following: The density of the RPC decreased with an increasing RA replacement ratio. The density of the RPC prepared with a double-gap-graded RA mix was lower than that prepared with a single-gap-graded RA (particle size: 10–20 mm) mix. The permeation coefficient of the RPC increased with increasing porosity. The splitting tensile strength of the RPC was positively correlated with its compressive strength. The compressive strength of the RPC decreased with increasing porosity. The regression analysis showed that the impact and abrasion resistance of the RPC increased with increasing compressive strength. In addition, all of the RPC specimens met the strength and permeation requirements. This study can provide theoretical support for the application of RPC.

Keywords: Recycled aggregate; recycled pervious concrete; strength; permeability; wear resistance; mix proportion

1 Introduction

Pervious concrete (PC) is a new type of environmentally friendly concrete. The research and application of PC began in the 1970s and 1980s in the United States. China is currently popularizing the use of PC extensively. Particularly, there will be a tremendous demand for this material in China for low impact development and construction. This means that large quantities of natural aggregates will be consumed.

Waste concrete blocks can be crushed, sieved, cleaned and graded and subsequently mixed at certain ratios to form recycled aggregates (RAs), which can then be used to replace natural aggregates in the



This work is licensed under a Creative Commons Attribution 4.0 International License, which permits unrestricted use, distribution, and reproduction in any medium, provided the original work is properly cited.

production of PC for road pavements. This approach can achieve effective recycling and reuse of large quantities of construction waste, alleviate increasing shortages of resources as a result of rapid economic development in China, ease the load on groundwater drainage facilities, mitigate the urban “heat island effects” and improve the environment. In addition, PC contains a relatively large number of pores and is thus able to absorb air pollutants and consequently reduce fugitive dust pollution and eliminate noise from vehicle operation [1]. From the perspective of sustainable development, the production of RA-containing PC (RPC) involves the recycling and reuse of renewable resources and is therefore harmonious with the natural ecosystem.

Research on the use of RAs in PC production is still at the early stage. Through experimentation, Güneyisi et al. [2] found that the tensile strength of PC decreased with an increasing RA replacement ratio. In contrast, Zaetang et al. [3] found that the tensile strength of PC increased to a small extent with an increasing RA replacement ratio within 60% and that the tensile strength of PC prepared with the RA replacement ratio of 100% was slightly lower than that of natural PC (NPC). Aliabdo et al. [4] found that use of 50% and 100% recycled aggregate generally yields splitting tensile strengths less than the recommended ranges and Addition of silica fume significantly enhances strength indices of pervious concrete where it is recommended to use 10% silica fume in case of using recycled aggregate in pervious concrete production. Xu et al. [5] found that pervious concrete using RCAs coated with TiO₂ could largely maintain its photocatalytic capacity. Zhu et al. [6] the results show that the permeability coefficient of the pervious concrete is the most suitable with a water-cement ratio of 0.30 and fiber can significantly improve the flexural strength of pervious concrete. In addition, Barnhouse et al. [7] also studied RPC through experimentation. These studies generally concluded that RPC met the basic performance requirements. However, these studies employed different methods and presented different views on the relationship between the RA replacement ratio and the performance of PC. In this study, the RA with gradations needed for the experiment was produced by mechanical crushing and sieving of demolished discarded concrete pavements. On this basis, the properties of the RA, as well as the strength, permeability and impact and abrasion resistance of RPC specimens prepared with various RA replacement ratios and RA gradations, were determined through tests.

2 Raw Materials and Test Methods

2.1 Raw Test Materials

The types and sources of the raw materials used in this study are as follows:

Cement: Tianrui P-O 42.5 ordinary Portland cement (see [Tab. 1](#) for its main physical properties).

Table 1: The physical and paste mechanical properties of cement

Project	Specific surface area (m ² /kg)	Density (kg/m ³)	Setting time (min)		Compressive strength (MPa)		Flexural strength (MPa)	
			Initial setting	Final setting	3 d	28 d	3 d	28 d
Result	348.7	3035	176	244	25.9	49.6	5.9	8.6

Coarse aggregates: The rock used is limestone with particle sizes of 10–20 mm was selected as the natural coarse aggregate. The RA was prepared by crushing (using a jaw crusher) and mechanical sieving of demolished discarded concrete pavements ([Fig. 1](#)). To investigate the effects of RA replacement ratio and gradation on RPC performance, RA particles with sizes of 10–20 and 5–10 mm were used ([Fig. 2](#)). Various physical properties of aggregates were investigated according to the Standard for technical requirements and test method of sand and crushed (or gravel) for ordinary concrete (JCJ52-2006) [8], [Tab. 2](#) shows the physical properties of aggregates.



Figure 1: Aggregate source



Figure 2: Regenerated coarse aggregate (10–20 mm)

Table 2: Physical properties of aggregates

performance index	Particle size range (mm)	Apparent density (kg/m ³)	Bulk density (kg/m ³)	Moisture content (%)	Crushing index	24h water absorption (by mass) (%)
natural aggregate	10–20	2727	1599	0.2	9.53	1.2
Recycled aggregate	10–20	2609	1381	4.23	15.54	5.7
	5–10	2559	1225	2.75	23.14	9.1

2.2 Mix Proportion Design

The water–cement ratio is of vital importance to the strength and permeability of RPC. An excessively high water–cement ratio will result in high fluidity and a thin cement paste layer on the aggregate surface with weak bonding strength, then the pervious concrete strength decreases. While an excessively low water–cement ratio can result in a thick cement paste layer and high strength, it will cause difficulty in molding

and compacting the mixture [9]. In this study, based on relevant specifications and the literature [10,11], the water–cement ratio was set to 0.30.

The mix proportions were designed by varying the RA replacement ratio (0, 25%, 50% and 75%) and gradation (particle size: 5–10 and 10–20 mm; mass ratio of RA particles with sizes of 5–10 mm to RA particles with sizes of 10–20 mm (hereinafter 5–10 mm/10–20 mm RA mass ratio): 1:1, 1:2, 2:1, 2:3 and 3:2). Tab. 3 shows the designed mix proportions.

Table 3: Proportions of all the concrete mixes used

Sample number	Substitution rate (%)	NCA (kg/m ³) (10–20mm)	RCA (kg/m ³)		Cement (kg/m ³)	Water (kg/m ³)
			(5–10 mm)	(10–20 mm)		
NPC	0	1474	0	0	328	98
RPC25	25	1106	0	369	328	98
RPC50	50	737	0	737	328	98
RPC75	75	369	0	1106	328	98
RPC1-1	100	0	737	737	328	98
RPC1-2	100	0	491	983	328	98
RPC2-1	100	0	983	491	328	98
RPC2-3	100	0	590	884	328	98
RPC3-2	100	0	884	590	328	98

Cubic (side length: 150 mm) and cylindrical (ϕ 100 mm \times 200 mm) specimens were prepared and cured in the laboratory. The concrete was mixed mechanically. The feeding sequence was as follows: Half of the mixing water was added into the coarse RA and the mixture was stirred for 1 min. Then, cement was added into the mixture, and the new mixture was mixed for 1 min. Finally, the remaining mixing water was added into the mixture, and the new mixture was mixed again for 2 min, after which the mixture was poured into molds to prepare specimens.

The molding method has a relatively significant impact on the PC performance [12]. Research has shown that PC specimens prepared by vibrating compaction exhibit the best performance with narrowly dispersed, uniformly distributed and highly repeatable pore sizes and no noticeably fragmented aggregate. Therefore, a method combining tamping with a tamper and vibrating compaction was employed in this study to mold the specimens [13]. For each mold, the concrete mix was first poured into the mold to half full, the slurry was subsequently tamped with a tamper 25 times, and then, the mold was vibrated on a vibrating table for 20 s; afterward, the concrete slurry was poured again into the mold to completely fill it, and the aforementioned molding process was repeated. Finally, a ϕ 40-mm iron rod was used to roll the molding surface until it was flat, and subsequently, a trowel was used to smooth the surface (Fig. 3).

2.3 Sample Maintaining

After the molding process, the specimens were placed in a shady and cool environment for 1 d. Afterward, the specimens were removed from the molds and placed in a standard curing chamber (temperature: $20 \pm 2^\circ\text{C}$; humidity: $>95\%$) for curing. After 28 d of curing, the specimens were tested to determine their porosity, permeation coefficient, compressive strength, splitting tensile strength and impact and abrasion resistance.

Each test group contained three specimens, and the measurements were averaged for analysis.



Figure 3: Specimen preparation and molding

2.4 Testing of the Permeability of the Specimens

2.4.1 Porosity

The effective porosity of each specimen was determined by calculating the difference between the mass of the specimen after being dried in the air until saturated surface dried and the mass of the specimen after being soaked in water for 24 h, using the following equation:

$$P = \left[1 - \frac{m_2 - m_1}{\rho_w V_0} \right] \times 100\% \quad (1)$$

where P is the porosity, %; m_1 is the mass of the specimen underwater, g; m_2 is the mass of the specimen after being dried in air for 24 h, g; V_0 is the volume of the specimen, cm^3 ; and ρ_w is the density of water at room temperature, g/cm^3 .

2.4.2 Permeation Coefficient

The permeation coefficient is an important index for evaluating the permeability of RPC. Most researchers measure the permeation coefficient using $\phi 100 \text{ mm} \times 200 \text{ mm}$ cylindrical specimens based on Darcy's law. Güneşiyisi et al. [2] measured the permeation coefficient using the falling head method. Sata et al. [5], Bhutta et al. [14] and Li et al. [15] measured the permeation coefficient using the constant head method based on the test method recommended by the Japan Concrete Institute [16]. In this study, cubic (side length: 150 mm) test specimens were used to determine the permeation coefficient. In addition, based on the existing research, a permeation coefficient measuring device (Fig. 4) was developed in-house based on Darcy's law and the constant head method. The permeation coefficient of each specimen was calculated using the following equation:



Figure 4: Permeation coefficient measuring device

$$k = \frac{VL}{AHt} \quad (2)$$

where k is the permeation coefficient, cm/s; V is the volume of water in the beaker within time t , cm³; L is the height of the specimen, mm; A is the surface area of the specimen, cm²; H is the head difference, cm; and t is the permeation time, s.

The surface of each RPC specimen was coarse and porous. Seepage from the sides of an RPC specimen would significantly affect the measurement of its permeation coefficient. Therefore, addressing the problem of seepage from the sides was the key to ensuring measurement accuracy. In this study, a cement paste was used to seal each specimen. The key to this method is to ensure a suitable consistency of the cement paste. If the cement paste is too thin, it will seep into the specimen, thereby blocking its pores and affecting its permeability. If the cement paste is too thick, it will be difficult to apply to the specimen. The mix proportion ratio of the cement paste is: *cement: water = 9:4 (by mass)*, the layer coat thickness less than 2 mm. Specifically, for each specimen, its four sides were coated with the selected cement paste, leaving only its top and bottom uncoated, which would subsequently serve as pervious surfaces. When applying the cement paste, no gaps were left at the edges and corners. In addition, to facilitate the removal process, each specimen was fixed with an L-shaped slot. Moreover, each cement paste-coated specimen was secured with rubber bands.

Each test group contained three specimens. Each specimen was tested three times within the same amount of time. The results were averaged.

2.5 Strength Performance

The RPC specimens were tested on a YAW6506 computer-controlled electro-hydraulic servo compression testing machine based on the Standard for test methods of concrete physical and mechanical properties (GB/T 50081-2019) [17] to determine their compressive strength and splitting tensile strength.

Test steps of compressive strength:

Take out the specimen from the curing room and place the specimen between the upper and lower pressing plate of the testing machine, so that the longitudinal axis of the specimen is consistent with the pressing plate center. Start the compression testing machine, add load continuously and uniformly until the failure of the specimen, and record the failure load F (N). The compressive strength of concrete should be calculated according to the following formula:

$$f_{cc} = \frac{4F}{\pi d^2} \quad (3)$$

where f_{cc} is compressive strength of concrete, MPa; F is failure load of the specimen, N; d is the calculated diameter of the specimen, mm.

Test steps of splitting tensile strength:

Remove the specimen from the curing room, wipe the pressure surface of the upper and lower pressure plates of the testing machine, place the cylinder specimen in the testing machine center, and add load continuously and evenly. The splitting tensile strength of cylinder is calculated as follows:

$$f_{ct} = \frac{2F}{\pi \times d \times l} = 0.637 \frac{F}{A} \quad (4)$$

where f_{ct} is Splitting tensile strength of cylinder specimen, MPa; F is failure load of the specimen, N; d is the diameter of the specimen with cleavage plane, mm; l is the height of specimen, mm; A is the fracture surface area of the specimen, mm².

2.6 Impact and Abrasion Resistance

The degradation test was conducted according to ASTM C1747 [18]. The Los Angeles abrasion test method, a method for measuring and evaluating the impact and abrasion resistance of coarse aggregates used in concrete for road and transit construction, was employed to determine the impact and abrasion resistance of the RPC specimens. From the material perspective, the impact and abrasion resistance of the aggregate and the bonding strength between the aggregate and the cement mortar are the main factors that affect the impact and abrasion resistance of RPC. When used to test the impact and abrasion resistance of the RPC specimens, the Los Angeles abrasion test method not only could determine the impact and abrasion resistance of the aggregate but also could reflect the bonding strength between the aggregate and the mortar.

Cylindrical test specimens ($\phi 100 \text{ mm} \times 150 \text{ mm}$) that had been cured for 28 d under standard conditions were used to determine the impact and abrasion resistance of the RPC based on the abrasion test method for coarse aggregates (i.e., the Los Angeles abrasion test method). The main device used for the abrasion test was an MH-II Los Angeles abrasion tester (inner diameter of the cylinder: $710 \pm 5 \text{ mm}$; inner length of the cylinder: $510 \pm 5 \text{ mm}$; rotational speed: 30–33 r/min; Fig. 5).



Figure 5: Los Angeles abrasion tester

The test procedure was as follows: (1) Specimens were dried in the air, and their initial masses, M_0 , were measured. (2) Three specimens were placed inside the steel cylinder at the same time, and the number of revolutions of the steel cylinder was set to x . Then, the tester was turned on. (3) After the steel cylinder stopped rotating, the tester was turned off, and the mass of each specimen, M_x , was measured. In this study, the number of revolutions was set to 500. The mass loss ratio, Q , after 500 impact and abrasion cycles, was used to represent the impact and abrasion resistance. The lower the mass loss ratio is, the higher the impact and abrasion resistance, and vice versa. The mass loss ratio was calculated using the following equation:

$$Q = \frac{M_0 - M_x}{M_0} \times 100\% \quad (5)$$

where Q is the mass loss ratio of the specimen, %; M_0 is the mass of the specimen before being subjected to impact and abrasion, g; and M_x is the mass of the specimen after x times of impact and abrasion, g.

3 Test Results and Analysis

The main performance indices of the RPC include strength, permeability and impact and abrasion resistance. The strength of the RPC is represented by its compressive strength and splitting tensile strength. The permeability of the RPC is represented by its porosity and permeation coefficient.

3.1 Density

Fig. 6 shows the effects of the RA replacement ratio and aggregate gradation on the density of the RPC. The test results show the following: (1) The density of the RPC was in the range of 1,730–1,960 kg/m³ and decreased with an increasing RA replacement ratio. This is in agreement with the results reported in reference [3]. (2) The RPC specimens prepared with a single-gap-graded RA mix each had a higher density than those prepared with a double-gap-graded RA mix. The RPC specimens prepared with a double-gap-graded RA mix with a 5–10 mm/10–20 mm RA mass ratio of 3:2 had the lowest density (1,732 kg/m³). This is because the old mortar was adhered to the RA surface, and consequently, the RA had relatively low apparent and bulk densities, which were approximately 90% of those of the natural aggregate. In addition, the RA particles with sizes of 5–10 mm had a bulk density of 1,225 kg/m³, which was approximately 88.7% of that of the RA particles with sizes of 10–20 mm. As a result, the density of a mixture containing small RA particles was relatively low.

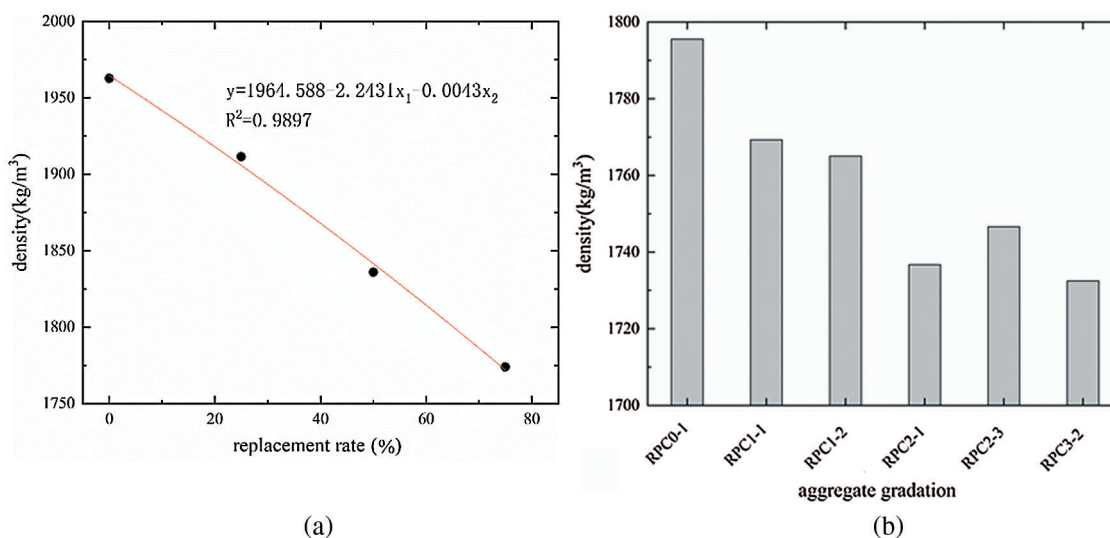


Figure 6: Effects of different substitution rates and aggregate gradation on RPC density

3.2 Analysis of the Permeability of the RPC

Tab. 4 shows the test results for the porosity and permeation coefficient of the RPC. In the American Concrete Institute (ACI) 522 Code [19], the porosity of RPC falls in the range of 15~35%. In this study, the porosity of the RPC was found to be in the range of 20.31%~23.83%, which is in line with the range specified in the ACI 522 code.

Güneyisi et al. [2] and Omary et al. [20] both found that the porosity of RPC increased with an increasing RA replacement ratio. Zaetang et al. [3] found that the porosity of RPC specimens prepared with various RA replacement ratios ranged from 23% to 25%, and the porosity of NPC specimens was 25%; in addition, they also found that the effects of the RA replacement ratio on the porosity of RPC were insignificant. In this study, no significant correlation was observed between porosity and RA replacement ratio. Compared to the NPC specimens, the RPC specimens prepared with an RA replacement ratio of 25% had the lowest

porosity (20.31%), and the RPC specimens prepared with an RA replacement ratio of 75% had the highest porosity (23.83%). This difference in results mainly occurs because the RAs used in different studies were obtained from different sources and differed in performance. In addition, as a result of the differences in the PC mix proportions and preparation techniques, the basic patterns reflected by the porosity measurements also vary among studies. The RPC specimens prepared with an RA mix with a 5–10 mm/10–20 mm RA mass ratio of 1:2 had the lowest porosity (18.85%). The RPC specimens prepared with an RA mix with a 5–10 mm/10–20 mm RA mass ratio of 3:2 had a relatively high porosity (23.14%).

Table 4: Porosity and permeability coefficient of recycled water-permeable concrete

Sample number	Porosity range (%)	Average porosity (%)	Permeability coefficient (mm/s)
NPC	20.33~22.87	21.99	4.13
RPC25	19.59~20.80	20.31	4.39
RPC50	19.14~22.87	21.23	3.67
RPC75	23.41~24.47	23.83	3.84
RPC1-1	19.35~23.70	21.48	3.74
RPC1-2	16.68~20.74	18.85	3.53
RPC2-1	22.22~26.34	22.44	3.86
RPC2-3	19.59~20.44	20.09	3.96
RPC3-2	21.78~25.19	23.14	4.20

Fig. 7 shows the relationship between porosity and permeation coefficient. Bhutta et al. [14] found that the permeation coefficient of PC linearly increased with increasing porosity within the range of 23–28%. Zaetang et al. [3] and Sata et al. [5] found a positive exponential correlation between permeation coefficient and porosity. The test results obtained in this study show that the permeation coefficient of the RPC was in the range of 3.28–4.39 mm/s and increased with increasing porosity, which is in agreement with the existing results. This is mainly because an increase in porosity results in an increase in the number of interconnected channels inside the RPC, an increase in the effective pervious area, a decrease in the resistance to water flow and an increase in the volume and rate of water flow, thereby resulting in an increase in permeability.

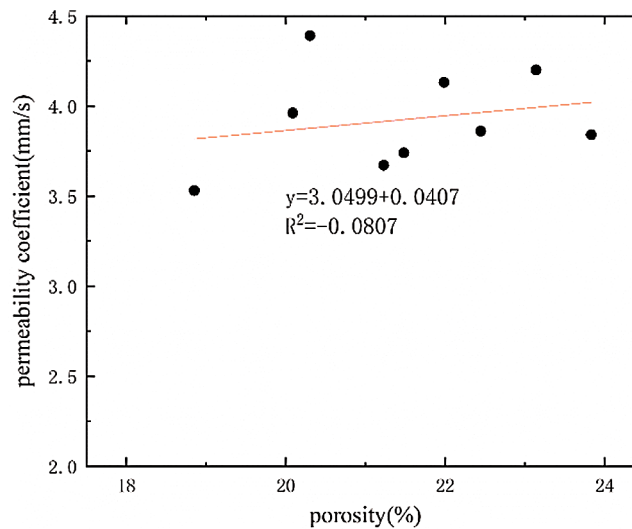


Figure 7: Relation between porosity and permeability coefficient

3.3 Strength Performance

Strength is an important parameter of PC. The use of RAs should provide sufficient strength to the PC [3]. In reference [19], the compressive strength of the PC specimens ranged from 2.8 to 28 MPa. In this study, the compressive strength of the specimens was found to fall in the range of 5.18~7.58 MPa, which is in agreement with the range specified in the ACI 522 Code.

Fig. 8 shows the compression failure of RPC specimens. As demonstrated in Fig. 8, cracks mainly propagated obliquely. In addition, the specimens were also crushed in a few local areas. Not only did bonding interface failure occur, but a relatively large number of aggregate particles were also fractured. Most of the fracture surfaces were formed as a result of the fracture of old mortar and the failure of interfacial transition zones (i.e., those between the natural aggregate and the new mortar or the old mortar).

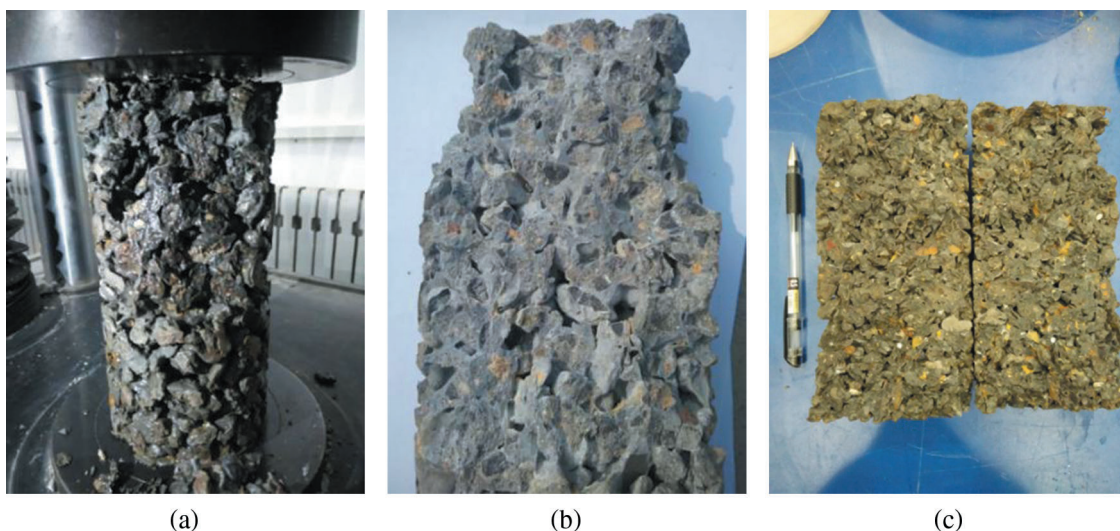


Figure 8: Compression and splitting failure of specimens. (a) Compressive strength test, (b) Compression failure of specimens, (c) splitting failure of specimens

PC has a skeleton–pore structure formed by mixing a coarse aggregate, cement and water and contains no sand. In addition, PC also contains a large number of pores, including both closed pores and interconnected pores. Therefore, the compression failure mechanism of PC differs from that of ordinary concrete [21]. When a load is applied to an RPC specimen, the set cement between RA particles is under shear stress. The closer the RA particles are to one another, the thinner the cement bonding layer between the RA particles is, the weaker this layer is, and the smaller the load this layer can bear. Therefore, the set cement between RA particles that are close to one another cracks first, and the cracks rapidly propagate and run through the set cement in this area until they connect to the pores in the specimen. Afterward, the cracks rapidly propagate to the surrounding particles. With the failure of the surrounding particles, the whole specimen eventually fails. In addition, RA particles have irregular shapes and non-uniform edges and corners. When a load is applied, due to stress concentration, RA particles fracture at the tips, resulting in their dislocation, which in turn results in a change in the mechanical conditions inside the specimen, causing it to fail as shown in Fig. 9. Moreover, the interface between the RA-containing old cement mortar and the original RA is relatively weak and is prone to fracture under loading.

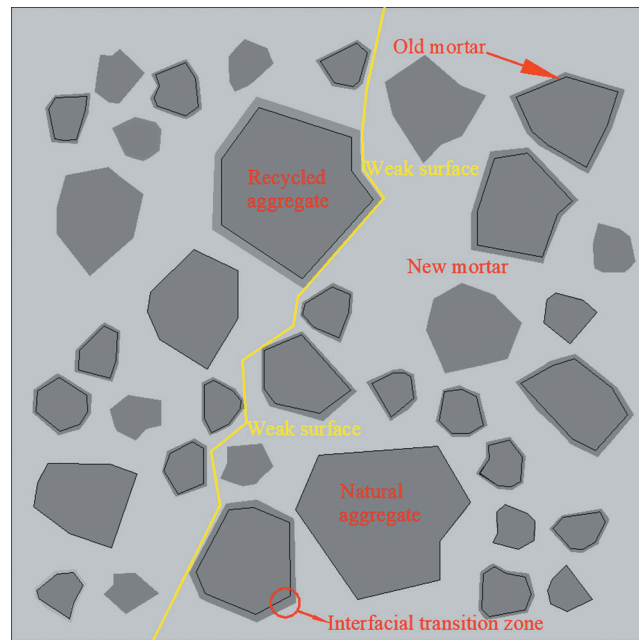


Figure 9: The schematic diagram of the failure mechanism of PRC under load

Fig. 10 shows the effects of the RA replacement ratio and RA gradation on the compressive strength of the RPC. The test results show the following: (1) The compressive strength of the RPC was higher than that of the NPC, which is in agreement with the findings reported in references [22–25]. This may be because the compressive strength of porous PC is mainly determined by the meshing friction between coarse aggregate particles and the bonding strength between the aggregate and the cement mortar [26]. Aggregate particles have rough surfaces. An increase in the meshing friction between aggregate particles or in the thickness of the cement mortar layer between aggregate particles results in an increase in the bonding strength, which in turn results in an increase in the compressive strength. In addition, during the mixing process, the water absorbed by the aggregate is released as cement hydration progresses. RPC can retain a certain amount of moisture inside it, which enables internal curing and facilitates the development of compressive strength [23]. (2) The compressive strength of the specimen RPC1-1 was lower than that of the specimens prepared with other RA gradations. The specimen RPC3-2 had relatively high compressive strength and splitting tensile strength.

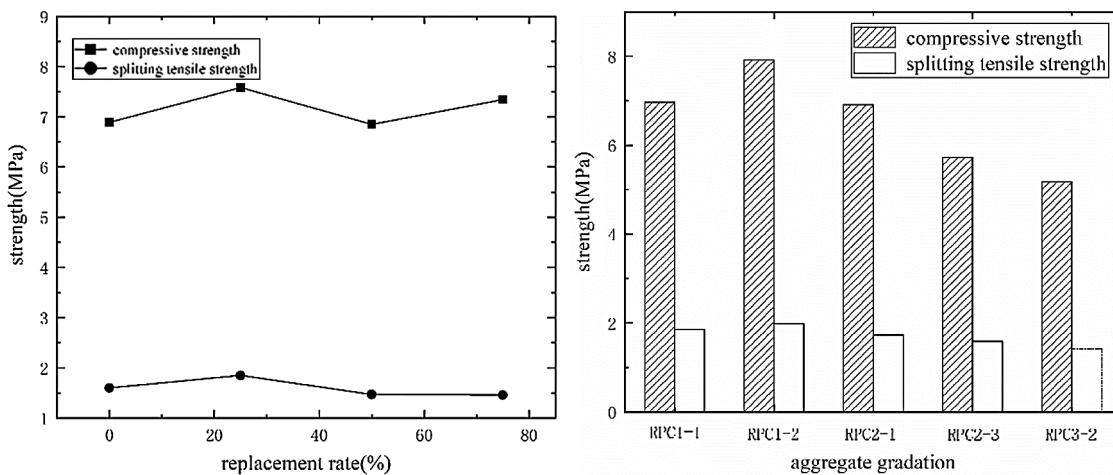


Figure 10: RPC the change rule of compressive strength under the influence of substitution rate and aggregate gradation

Fig. 11 shows the relationship between the compressive strength and splitting tensile strength of the RPC. The splitting tensile strength of the RPC increased with increasing compressive strength, which is in line with the description in the ACI318 code [27]. However, the measurements of the splitting tensile strength of the RPC obtained in this study are slightly higher than those specified in the ACI 318 code. In references [28,29], the tension–compression ratio of NPC specimens was found to fall in the range of 9~14%. In this study, the tension–compression ratio of the RPC specimens was found to fall in the range of 20~28%, which is significantly higher than the range reported in references [28,29]. This suggests that the RPC specimens prepared in this study had lower brittleness and higher toughness than the NPC specimens studied in references [28,29].

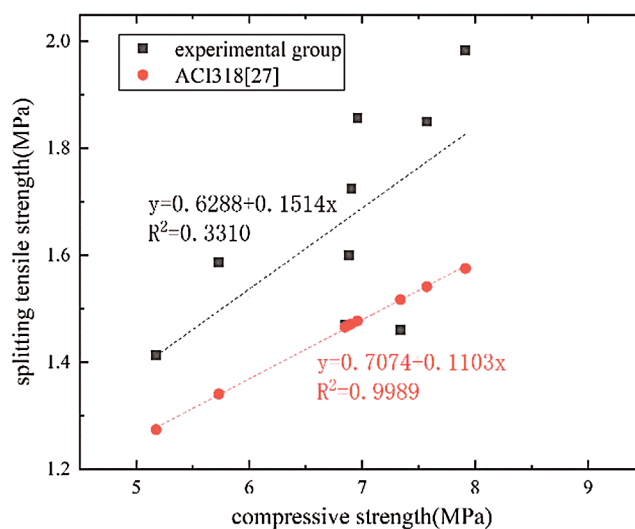


Figure 11: The relationship between compressive strength and splitting tensile strength

Fig. 12 shows the relationship between porosity and compressive strength. Bhutta et al. [14] found that the compressive strength of PC almost linearly decreased with increasing porosity within the range of 23–28%. Sriravindrarajah et al. [11] found an exponential relationship between compressive strength and porosity and that the compressive strength decreased with increasing porosity. The relationship between the compressive strength and porosity of the RPC found in this study is basically in agreement with that found in reference [14]: the compressive strength of the RPC decreased linearly with increasing porosity. This may be because the more pores there are in the RPC, the more significant the resultant stress concentration and, consequently, the lower the compressive strength of the RPC.

3.4 Abrasion Resistance

Specimens were prepared based on the RPC mix proportions shown in Tab. 3. After 28 d of curing, the compressive strength and mass loss ratio of the specimens were tested after 500 impact and abrasion cycles. Figs. 13 and 14 show the specimens before and after being subjected to 500 impact and abrasion cycles, respectively.

Fig. 15 shows the mass loss ratios of the RPC specimens prepared with various RA replacement ratios and RA gradations after 500 impact and abrasion cycles. As demonstrated in Fig. 15, the mass loss ratio of specimen RPC25 was lower than those of the other specimens, indicating that specimen RPC25 had high impact and abrasion resistance. Moreover, the specimens prepared with a double-gap-graded RA mix each had a relatively higher mass loss ratio. Specimen RPC3-2 had the highest mass loss ratio (30.57%).

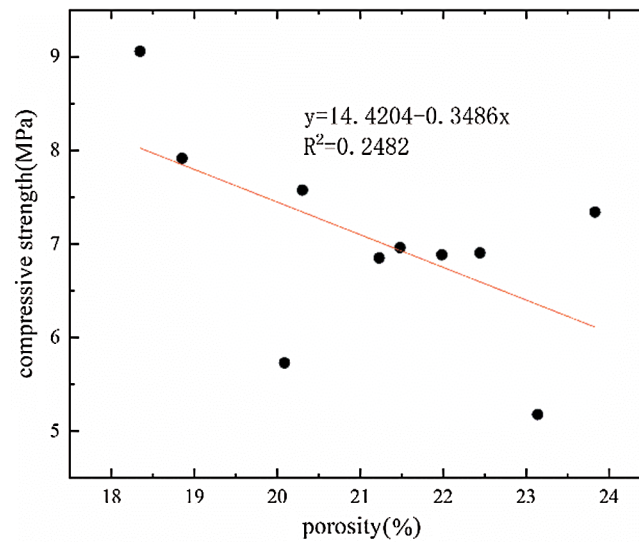


Figure 12: The relationship between porosity and compressive strength



Figure 13: Specimens before the impact and abrasion test

The impact and abrasion resistance of PC relies on its compressive strength. In addition, the water–cement ratio is also a main factor that affects the impact and abrasion resistance of PC. The lower the water–cement ratio is, the higher the compressive strength and the higher the impact and abrasion resistance [30,31]. Fig. 16 shows the relationship between the compressive strength and impact and abrasion resistance of the RPC. The regression analysis [32] shows a power function ($y = 69.2554x^{-0.5160}$, $R^2 = 0.8461$) relationship between the mass loss ratio of the RPC after 500 impact and abrasion cycles and its compressive strength. Therefore, the impact and abrasion-induced mass loss ratio of PC can be estimated based on its compressive strength. This provides a reference basis for the application of RPC in engineering practice.



Figure 14: Specimens after 500 impact and abrasion cycles

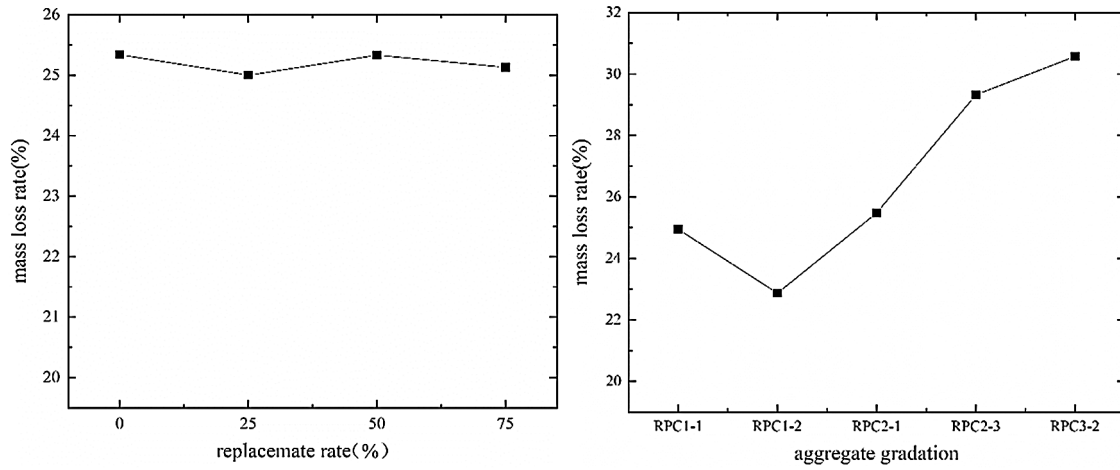


Figure 15: Mass loss rates of different substitution rates and gradation wear rates

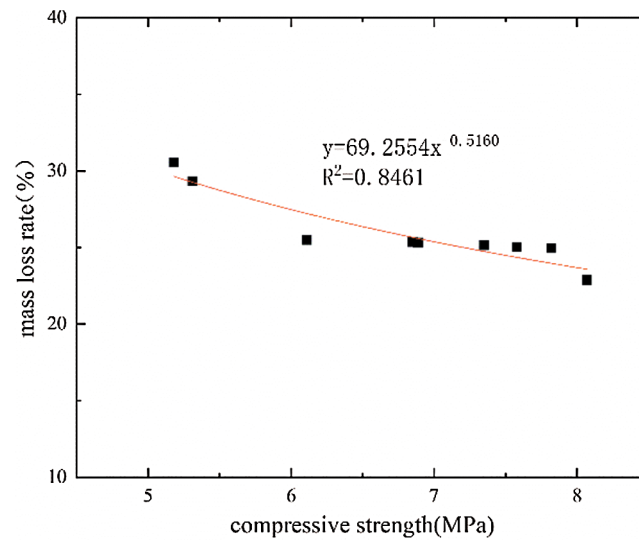


Figure 16: The relationship between the mass loss rate of the impact wear and the compressive strength

4 Conclusions

In this study, the RA was obtained by mechanical crushing and sieving demolished discarded concrete pavements and was subsequently tested and analyzed. On this basis, the effects of the RA replacement ratio and RA gradation on the strength and permeability of the RPC were investigated. The main conclusions derived from this study are summarized as follows:

(1) Compared to the natural aggregate, the RA had relatively lower bulk and apparent densities. The density of the RPC decreased with an increasing RA replacement ratio. The RPC specimens prepared with a single-gap-graded RA mix each had a higher density than those prepared with a double-gap-graded RA mix.

(2) There was no significant correlation between the RA content and porosity of the RPC, The RPC specimens prepared with an RA replacement ratio of 25% had the lowest porosity, whereas the RPC specimens prepared with an RA replacement ratio of 75% had the highest porosity. However, the permeation coefficient of the PRC increased noticeably with increasing porosity. In addition, specimen RPC1-2 had a higher compressive strength but lower porosity and permeability than the other specimens prepared with a double-gap-graded RA mix. Specimen RPC3-2 had relatively high porosity and permeation coefficient but relatively low compressive strength.

(3) Compared to the NPC, the RPC specimens prepared with an RA replacement ratio of 25% had a significantly higher compressive strength (7.58 MPa). A positive correlation was found between the splitting tensile strength and the compressive strength of the RPC. The tension–compression ratio of the RPC fell in the range of 20~28%. In addition, there was a basically negative correlation between the compressive strength and porosity of the RPC—The compressive strength decreased with increasing porosity.

(4) The RPC specimens prepared with an RA replacement ratio of 25% had the lowest mass loss ratio (25%). In addition, the RPC specimens prepared with a single-gap-graded RA mix each had a lower mass loss ratio than those prepared with a double-gap-graded RA mix, suggesting that the RPC specimens prepared with a single-gap-graded RA mix had relatively high impact and abrasion resistance. Moreover, the regression analysis showed that the mass loss ratio of the RPC decreased with increasing compressive strength. In other words, the impact and abrasion resistance of the RPC increased with increasing compressive strength. There was a power function ($y = 69.2554x^{-0.5160}$, $R^2 = 0.8461$) relationship

between the mass loss ratio and compressive strength of the RPC. Hence, the impact and abrasion resistance of RPC can be estimated based on its compressive strength.

Funding Statement: This study was funded by the National key research and development program fund project (No. 2018YFC0406803).

Conflicts of Interest: The authors declare that they have no conflicts of interest to report regarding the present study.

References

1. Ngohpok, C., Sata, V., Satiennam, T., Klungboonkrong, P., Chindapasirt, P. et al. (2018). Mechanical properties, thermal conductivity, and sound absorption of pervious concrete containing recycled concrete and bottom ash aggregates. *KSCE Journal of Civil Engineering*, 22(4), pp. 1369–1376. DOI 10.1007/s12205-017-0144-6.
2. Güneysi, E., Gesoğlu, M., Kareem, Q., Suleyman, I. (2016). Effect of different substitution of natural aggregate by recycled aggregate on performance characteristics of pervious concrete. *Materials & Structures*, 49(1-2), 521–536.
3. Zaetang Y., Sata V., Wongs A., Chindapasirt P. (2016). Properties of pervious concrete containing recycled concrete block aggregate and recycled concrete aggregate. *Construction and Building Materials*, 111, 15–21.
4. Aliabdo, A. A., Abd Elmoaty, A. E. M., Fawzy, A. M. (2018). Experimental investigation on permeability indices and strength of modified pervious concrete with recycled concrete aggregate. *Construction and Building Materials*, 193, 105–127. DOI 10.1016/j.conbuildmat.2018.10.182.
5. Xu, Y. D., Jin, R. Y., Hu, L., Li, B., Chen, W. et al. (2020). Studying the mix design and investigating the photocatalytic performance of pervious concrete containing TiO₂-Soaked recycled aggregates. *Journal of Cleaner Production*, 248, 119281. DOI 10.1016/j.jclepro.2019.119281.
6. Zhu, H. T., Wen, C. C., Wang, Z. Q., Li, L. (2020). Study on the permeability of recycled aggregate pervious concrete with fibers. *Materials*, 13(2), 321. DOI 10.3390/ma13020321.
7. Barnhouse, P. W., Srubar, W. V. (2016). Material characterization and hydraulic conductivity modeling of macroporous recycled-aggregate pervious concrete. *Construction and Building Materials*, 110, 89–97. DOI 10.1016/j.conbuildmat.2016.02.014.
8. Standard for Technical Requirements and Test Method of Sand and Crushed (or Gravel) for Ordinary Concrete (2006). Ministry of Housing and Urban-Rural Development of the People's Republic of China. Beijing, China Building Industry Press, vol. JCJ52-2006.
9. Huang, B., Wu, H., Shu, X., Burdette, E. G. (2010). Laboratory evaluation of permeability and strength of polymer-modified pervious concrete. *Construction and Building Materials*, 24(5), 818–823. DOI 10.1016/j.conbuildmat.2009.10.025.
10. Zhang, X. X., Yin, J., Chi, Y. (2010). Review of pervious concrete properties. *Concrete*, 12, 47–50. DOI 10.3969/j.issn.1002-3550.2010.12.015.
11. Sriravindrarah, R., Wang, N. D. H., Lai, J. W. E. (2012). Mix design for pervious recycled aggregate concrete. *International Journal of Concrete Structures and Materials*, 6(4), 239–246. DOI 10.1007/s40069-012-0024-x.
12. Xu, R. C., Gui, M. M., Gong, M. Z., Liu, J. X., Chen, Q. J. (2012). Influence of different molding methods on pervious concrete properties. *Concrete*, 11, 129–131. DOI 10.3969/j.issn.1002-3550.2011.11.041.
13. Du, X. Q. (2016). *Experimental study on pervious concrete made from recycled aggregate*. Beilin: Xi'an University of Technology. <https://doi.org/CNKI:CDMD:2.1017.853299>.
14. Bhutta, M. A. R., Hasanah, N., Farhayu, N., Hussin, M. W., Tahir, M. B. M. et al. (2013). Properties of porous concrete from waste crushed concrete (recycled aggregate). *Construction and Building Materials*, 47, 1243–1248. DOI 10.1016/j.conbuildmat.2013.06.022.
15. Li, Q. S., He, D. P. (2013). Comparison test of natural and recycled aggregate permeable concrete. *Journal of Beijing University of Technology*, 41(1), 89–94. DOI 10.11936/bjtxb2014060062.
16. Japan Concrete Institute (2004). Construction and recent applications of porous concrete. *Proceedings of the JCI Symposium on Design, Tokyo*, pp. 1–10. Japan Concrete Institute.

17. GB/T 50081-2019 (2019). Standard for Test Methods of Concrete Physical and Mechanical Properties. China: Ministry of construction of People's Republic of China.
18. ASTM C1747/C1747M-13 (2013). *Standard test method for determining potential resistance to degradation of pervious concrete by impact and abrasion*. West Conshohocken, Pennsylvania, US, the ASTM Committee on Standards. Annual Book of ASTM Standard.
19. ACI 522R-10 (2010). *Pervious concrete*. Farmington Hills: American Concrete Institute Committee.
20. Omary, S., Ghorbel, E., Wardeh, G. (2016). Relationships between recycled concrete aggregates characteristics and recycled aggregates concretes properties. *Construction and Building Materials*, 108, 163–174. DOI 10.1016/j.conbuildmat.2016.01.042.
21. Wang, C. F., Liu, D. F., Zhu, Q. S. (2010). Experimental analysis of failure mechanism of highly permeable eco concrete. *Concrete*, 10, 50–52. DOI 10.3969/j.issn.1002-3550.2010.10.016.
22. Ridzuan, A. R. M., Diah, A. B. M., Hamir, R., Kamarulzaman, K. B. (2001). The influence of recycled aggregate on the early compressive strength and drying shrinkage of concrete. *Structural Engineering Mechanics and Computation*, 2, 1415–1422. DOI 10.1016/B978-008043948-8/50158-2.
23. Peng, G. F., Shen, D. Q., Zhu, H. Y., Liu, X. S. (2006). Comparison of mechanical properties of recycled aggregate concrete and base concrete under the condition of the same mixture ratio. *Concrete*, 2, 34–38. DOI 10.3969/j.issn.1002-3550.2006.02.011.
24. Xiao, J. Z., Li, J. B., Sun, Z. P., Hao, X. M. (2004). Study on compressive strength of recycled aggregate concrete. *Journal of Tongji University*, 32(12), 1558–1561. DOI 10.3321/j.issn:.
25. Li, J. B., Xiao, J. Z., Sun, Z. P. (2005). Characteristics of recycled coarse aggregate and their effects on the properties of recycled aggregate concrete. *Journal of Building Materials*, 17(5), 390–395. DOI 10.3969/j.issn.1007-9629.2004.04.006.
26. Jiang, Z. W., Sun, Z. P., Wang, P. M. (2005). Influence of several factors on the performance of porous pervious concrete. *Journal of Building Materials*, 8(5), 513–519. DOI 10.3969/j.issn.1007-9629.2005.05.008.
27. ACI 318 (1999). ACI committee 318. Building code requirements for structural concrete and commentary (ACI 318R-99). Detroit, USA: American Concrete Institute.
28. Kevern, J. T., Wang, K., Schaefer, V. R. (2010). Effect of coarse aggregate on the freeze-thaw durability of pervious concrete. *Journal of Materials in Civil Engineering*, 22(5), 469–475. DOI 10.1061/(ASCE)MT.1943-5533.0000049.
29. Kuo, W. T., Liu, C. C., Su, D. S. (2013). Use of washed municipal solid waste incinerator bottom ash in pervious concrete. *Cement and Concrete Composites*, 37(1), 328–335. DOI 10.1016/j.cemconcomp.2013.01.001.
30. Feng, C. W., Li, S. S., Qin, H. G., Yang, S., Wang, D. Y. (2008). Factors affecting the impact resistance and impact wear properties of concrete for lock chamber walls. *Concrete and Cement Products*, 2, 38–41. DOI 10.3969/j.issn.1000-4637.2008.02.011.
31. Feng, C. W. (2008). *Study on crack resistance and impact wear resistance of high performance concrete for lock chamber wall*. Nanjing, China: Southeast University.
32. Pang, C. M., Qin, H. G., Ji, J. (2000). *Experimental design and concrete nondestructive testing technology*. Beijing, China Building Materials Press.